Dalton Transactions

Construction of Polyoxometalates from Dynamic Lacunary Polyoxotungstate Building Blocks and Lanthanide Linkers

Journal:	*Dalton Transactions*
Manuscript ID:	DT-ART-02-2015-000686.R2
Article Type:	Paper
Date Submitted by the Author:	05-May-2015
Complete List of Authors:	Li, Lulu; Northeast Normal University, Department of Chemistry Han, Hua-Yan; The Key laboratory of Polyoxometalate Science of Ministry of Education, Faculty of Chemistry Wang, Yong-Hui; Northeast Normal University, Department of Chemistry Tan, Huaqiao; Changchun Institute of Optics, Fine Mechanics and Physics, State Key Laboratory of Luminescence and Applications Zang, Hong-Ying; The Key laboratory of Polyoxometalate Science of Ministry of Education, Faculty of Chemistry, Department of Chemsitry Li, Yang-Guang; The Key laboratory of Polyoxometalate Science of Ministry of Education, Faculty of Chemistry

Dalton Transactions

Dynamic Article Links ►

Cite this: DOI: 10.1039/c0xx00000x

www.rsc.org/xxxxxx

Full Paper

Construction of Polyoxometalates from Dynamic Lacunary Polyoxotungstate Building Blocks and Lanthanide Linkers

Lu-Lu Li,[a] Hua-Yan Han,[a] Yong-Hui Wang,*[a] Hua-Qiao Tan,[a] Hong-Ying Zang,*[a] and Yang-Guang Li[a]

Received (in XXX, XXX) Xth XXXXXXXXX 20XX, Accepted Xth XXXXXXXXX 20XX

DOI: 10.1039/b000000x

Abstract

A series of polynuclear metal-oxo clusters are constructed from the dynamic polyoxometalate (POM) building block {B-α-$Sb^{III}W_9O_{33}$} and the lanthanide (Ln) linkers *via* the stepwise synthetic strategy with the molecular formula of $[Ln_2(H_2O)_4\{WO_2(pic)\}_2(SbW_8O_{30})_2]^{10-}$ (Na_4Li_6**[La-1]**·$28H_2O$, Na_3Li_7**[Pr-2]**·$30H_2O$) and $[\{Ln(H_2O)\}\{Ln(pic)\}(Sb_3O_4)(SbW_8O_{31})(SbW_{10}O_{35})]_2^{24-}$ ($K_2Na_6Li_{16}$**[Tb-3]**·$63H_2O$, Na_9Li_{15}**[Dy-4]**·$61H_2O$, Na_7Li_{17}**[Ho-5]**·$53H_2O$) (Hpic = picolinic acid). The five compounds have been characterized by FT-IR, elemental analysis, TG, powder X-ray diffraction (PXRD) and single crystal X-ray diffraction. In compounds **1-5**, various POM moieties such as {B-*β*-SbW_8O_{30}}, {B-α-SbW_8O_{31}} and {B-α-$SbW_{10}O_{35}$} are formed through a series of disassembling and re-assembling process of the dynamic {B-α-SbW_9O_{33}} precursor within specific pH, reaction temperature and time. Furthermore, the use of oxytropic Ln^{3+} ions as linkers, together with auxiliary organic pic ligands and/or inorganic Sb^{3+} ions, led to diverse connection modes between POM building blocks and Ln linkers and the assembly of new polynuclear metal-oxo clusters. The polyoxoanions of **La-1** and **Pr-2** possess the same structural feature, which can be viewed as a sandwich-type cluster composed of two {B-*β*-SbW_8O_{30}} units connected by two {WO_2(pic)} fragments and two hydrated Ln ions. Such sandwich-type polyoxoanions are further linked by the hydrated Ln ions to form a 1-D helical chain. The polyoxoanions of **Tb-3**, **Dy-4** and **Ho-5** display the same structural feature, although they contain different counter cations and lattice water molecules. In the polyoxoanions of **3-5**, one {B-α-SbW_8O_{31}} POM moiety and one {B-α-$SbW_{10}O_{35}$} POM unit are connected by one {Sb_3O_4} fragment and one {Ln(pic)} linker, forming an asymmetric sandwich-type metal-oxo cluster. Two of such sandwich-type clusters are further fused together by extra two hydrated Ln ions, leading to an isolated polynuclear metal-oxo cluster with the size of 16.4 × 28.5 Å. The photoluminescent properties of **Tb-3** and **Dy-4** were investigated. Both compounds exhibit characteristic Tb^{3+} and Dy^{3+} luminescence, respectively. The relationship between the luminescent property and the crystal structure of the polyoxoanion was discussed.

Introduction

The design and construction of polynuclear metal-oxo clusters based on polyoxometalates (POMs) have been paid much attention in recent years. The research on such polynuclear metal-oxo clusters have not only dramatically developed new POM structural systems,[1-4] but also provided an important molecular platform for the exploration of new photoluminescent nanoclusters, single-molecular magnets, light-induced water splitting catalysts, microporous materials, soluble inorganic nanocapsules, and nano-alloy catalysts.[5-10] In this research field, various synthetic strategies including one-pot synthesis, step-by-step method and "3-D printing" technique have been explored.[11-13] In any case, two basic building blocks can be found from final clusters, that is, various lacunary POM units and a series of linkers. Therefore, construction of POM-based polynuclear clusters can be viewed as a successive coexisting, activating and assembling process happened in the reaction system containing various POM building units and linkers. Usually, the above process will be realized by the control of various reaction conditions such as pH, reaction time, temperature, ionic strength and so on. During the synthesis of POM-based polynuclear metal-oxo clusters, the primary factor is the choice and introduction of dynamic lacunary POM precursors. Trivacant Keggin-type cluster {B-α-XW_9O_{33}} (X = As^{III}, Sb^{III}, Bi^{III}, Se^{IV}, Te^{IV}) containing the central distorted tetrahedral unit {XO_3} displays a great advantage in this field due to its several features as follows:[14-26] Firstly, {XW_9O_{33}} is highly vacant and can coordinate with multiple metal ions in various modes; Secondly, the central heteroatoms have a lone pair of electrons posing outside, which can somewhat avoid lacunary POM species from being saturated at a certain pH value and keep the coordination abilities to TM or Ln ions. Thirdly, the {B-α-XW_9O_{33}} species can be easily synthesized with a quite high yield. The most important of all, such {B-α-XW_9O_{33}} species can usually experience a structural isomerization, disassembling and re-assembling process, forming many active POM intermediates for the assembling of new polynuclear metal-oxo clusters. So far, several huge metal-oxo clusters with more than one hundred W centers are based on such trivacant {XW_9O_{33}} precursors.[11, 27-29] Moreover, it is also very important to choose suitable linkers, which should not only co-exist with various POM building blocks, but also possess suitable activity to react with the POM units in the reaction system. In this aspect, Ln^{3+} ions represent an ideal linking candidate due to their oxytropic property, various coordination modes, and Lewis acid feature.[12] Furthermore, their natural luminescent activity may also endow the clusters new functionalities. However, Ln^{3+} ions are sometimes over-reactive with POM precursors, leading to not crystallization but quick precipitates. The introduction of auxiliary organic and/or inorganic ligands has recently been developed that can somewhat slow down the quick reactions between two precursors.[22-26] In last decade, plenty of metal-oxo clusters based on {$As^{III}W_9O_{33}$} and Ln^{3+} linkers have been reported, in which an interesting synthetic trend has been observed, that is, the introduction of different auxiliary organic ligands will usually induce new Ln-POM assemblies and/or aggregates. In comparison, the metal-oxo

clusters based on $\{Sb^{III}W_9O_{33}\}$, Ln^{3+} ions and auxiliary organic/inorganic ligands have still been unexplored.[30,31] Considering that the bond lengths Sb^{III}-O are longer than those of As^{III}-O, together with the different chemical activities between As_2O_3 and Sb_2O_3, it is worth exploring new metal-oxo clusters based on the $\{Sb^{III}W_9O_{33}\}$ POM precursors and discovering the assembling change induced by the difference of central heteroatoms of the POM building blocks.

Based on aforementioned consideration, we have attempted to explore new polynuclear metal-oxo clusters by the use of the reaction system containing {B-α-SbW_9O_{33}} precursors, Ln^{3+} ions, organic picolinic acid (Hpic), and/or inorganic Sb^{3+} ions. Herein, we report five new compounds, $[Ln_2(H_2O)_4\{WO_2(pic)\}_2(SbW_8O_{30})_2]^{10-}$ (Na_4Li_6**[La-1]**$\cdot 28H_2O$, Na_3Li_7**[Pr-2]**$\cdot 30H_2O$), and $[\{Ln(H_2O)\}\{Ln(pic)\}(Sb_3O_4)(SbW_8O_{31})(SbW_{10}O_{35})]_2^{24-}$ ($K_2Na_6Li_{16}$**[Tb-3]**$\cdot 63H_2O$, Na_9Li_{15}**[Dy-4]**$\cdot 61H_2O$, Na_7Li_{17}**[Ho-5]**$\cdot 53H_2O$). The polyoxoanions of **La-1** and **Pr-2** possess the same structural feature, exhibiting a sandwich-type metal-oxo cluster composed of two {B-β-SbW_8O_{30}} units connected by two $\{WO_2(pic)\}$ fragments and two hydrated Ln ions. Such sandwich-type polyoxoanions are further linked by the hydrated Ln ions to form a 1-D helical chain. The polyoxoanions of **Tb-3**, **Dy-4** and **Ho-5** display the same structural feature, in which one {B-α-SbW_8O_{31}} and one {B-α-$SbW_{10}O_{35}$} POM unit are connected by one $\{Sb_3O_4\}$ fragment and one {Ln(pic)} linker, forming an asymmetric sandwich-type metal-oxo cluster. Two of such sandwich-type clusters are further fused together by extra two hydrated Ln ions, leading to an isolated metal-oxo cluster with size of 16.4 × 28.5 Å. To our knowledge, both polyoxoanions represent new type of metal-oxo clusters based on $\{SbW_9O_{33}\}$ species. The photoluminescent properties of **Tb-3** and **Dy-4** were investigated and both compounds exhibit the characteristic Tb^{3+} and Dy^{3+} luminescence, respectively.

Results and discussion

Synthesis

Two main synthetic strategies, that is step-by-step synthesis and one-pot reaction, have been employed to produce Ln-POM-based polynuclear metal-oxo clusters and aggregates. The former one involves the synthesis of various POM synthons first and then the assembly of POM synthons with Ln linkers. The latter one is combining various simple precursors such as WO_4^{2-}, Sb_2O_3, Ln^{3+} ions and organic ligands altogether in specific pH, reaction temperature, and ion strength. We have tried both strategies, but only the step-by-step synthetic strategy is suitable for the preparation of compounds **1-5** in this case. During the synthesis, the freshly prepared $Na_9[SbW_9O_{33}]$ synthons experienced an important disassembly and reassembly process, releasing extra $\{WO_6\}$ fragments to connect with the lacunary POM moieties. Furthermore, the partially disassembled POM species possessed high activity to react with Ln^{3+} ions and the organic ligands, exhibiting various linking modes. In this reaction system, some important reaction factors should be emphasized: (i) Only the use of freshly prepared $Na_9[SbW_9O_{33}]\cdot 19.5H_2O$ precursor can undergo a relatively quick precipitation and redissolving process. Furthermore, the use of fresh $Na_9[SbW_9O_{33}]\cdot 19\cdot 5H_2O$ precursor can improve the yields of crystalline products **1-5**; (ii) The 2:1 molar ratio of pic ligand to Ln^{3+} ions can utmostly protect Ln^{3+} ions from hydrolyzing or over-reacting with the POM anions, which usually leads to irreversible precipitate; (iii) When another assembly species Sb_2O_3 was introduced into the system, the concentrated hydrochloric acid was indispensable for dissolving such oxide precursor, generating the $\{Sb_3O_4\}$ linking moieties, and assembling compounds **3-5**; (iv) LiCl is vital to enhance the ion strength of the whole reaction system and cannot be substituted by other inorganic salts (*eg*. NH_4Cl, KCl, NaCl). It is initially presumed that the Li^+ ions may partially increase the solubility of the whole POM clusters, since the addition of other inorganic salts just led to quick precipitation in 24 h; (v) The Hpic ligand possesses a relatively high *p*Ka value of ca. 4.95, which can deprotonate into pic^- ligand in pH > 5 conditions. Such pic^- species can not only act as chelate ligand to coordinate with Ln and/or W centers, but also decrease the positive charge of {M-pic} fragments, providing suitable linkers to connect POM building units together.

In order to explore various experimental parameters that affect the final quality and yields of the crystalline metal-oxo assemblies, we performed a series of parallel experiments varying reaction time, pH and temperature (Table S1). Based on the parallel experiments, we found that the pH should range from 4.8 to 5.2 in the reaction system of compounds **1-2**, while the pH should be in the range of 6.3-6.7 in the reaction system of compounds **3-5**. Moreover, the reaction temperature and time were also optimized so as to improve the final quality and yields of the crystalline compounds. It was found that the 90 °C reaction temperature and 3 h reaction time are suitable for compounds **1-2**, while the 90 °C and 1 h are better for compounds **3-5**. In addition, capillary electrophoresis experiment[32] was conducted to initially prove the existence of the discovered POM cluster in solution under modified synthetic conditions. Such technique has been designed to separate species based on their charge to size ratio in the interior of a small capillary filled with an electrolyte. Herein, compounds **1** and **3** were chosen as representative samples to be investigated. In both measurements, the peak signals originated from the optimum synthetic systems of **1** and **3** were compared with those from the aqueous solution dissolving **1** and **3**, respectively. As shown in Fig. S1, the main peak appeared in optimum synthetic condition was same as the one of the corresponding compound, proving that the corresponding polyoxoanions of compound **1** and **3** are main species in the optimum synthetic solution system, respectively.

Based on the above experiment and the final structures of compounds **1-5**, we proposed that, in the preparation of compounds **1-2**, the initial lacunary POM building block B-α-$\{SbW_9O_{33}\}$ might experience a structural transformation and partial dissembling process, inducing new building units B-β-$\{SbW_8O_{30}\}$ and $\{WO_2(pic)\}$ (as shown in Scheme 1a and equation 1). In the synthesis of compounds **3-5**, the initial POM units B-α-$\{SbW_9O_{33}\}$ might just undergo partial dissembling and reassembling process, leading to B-α-$\{SbW_8O_{31}\}$ and B-α-$\{SbW_{10}O_{35}\}$ building blocks (as shown in Scheme 1b and equation 2-4).

$$[SbW_9O_{33}]^{9-} + H_2O = [SbW_8O_{30}]^{9-} + WO_4^{2-} + 2H^+ \quad (1)$$

$$[SbW_9O_{33}]^{9-} + 2H_2O = [SbW_8O_{31}]^{11-} + WO_4^{2-} + 4H^+ \quad (2)$$

$$[SbW_9O_{33}]^{9-} + WO_4^{2-} + 4H^+ = [SbW_{10}O_{35}]^{7-} + 2H_2O \quad (3)$$

$$2[SbW_9O_{33}]^{9-} = [SbW_8O_{31}]^{11-} + [SbW_{10}O_{35}]^{7-} \quad (4)$$

Thus, the relatively long reaction time may be necessary for the structural transformation, dissembling and reassembling process in the synthesis of compounds **1-2**. Moreover, other lanthanide ions were also attempted to introduce into the above two reaction systems, but the high quality of crystalline compounds have not been obtained yet. It is presumed that the

ionic radius and/or coordination modes of different Ln ions may influence the assembly process and crystallization in both reaction systems.

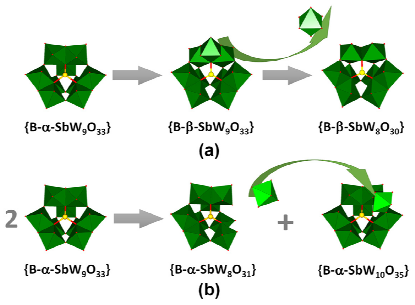

Scheme 1 Schematic view of the possible structural isomerization, dissembling and/or re-assembling processes in the synthesis of compounds **1-2 (a)** and **3-5 (b)**

Structure description

Single-crystal X-ray diffraction analyses confirm that compounds **1-2** crystallize in the orthorhombic space group $P2_12_12_1$. Herein, the structure of compound **1** was described as the representative example. Compound **1** contains a sandwich-type polyoxoanion unit $[La_2(H_2O)_4(WO_2(pic))_2(SbW_8O_{30})_2]^{10-}$ (Fig. 1). Such a POM unit consists of two $\{SbW_8O_{33}\}$ lacunary POM fragments, two metal-organic $\{WO_2(pic)\}$ moieties, one $\{La(H_2O)_3\}$ and one

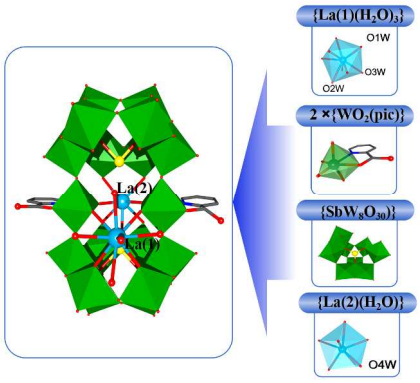

Fig. 1 Polyhedral and ball-and-stick view of the polyoxoanion structural unit of **1** and its basic building moieties

$\{La(H_2O)\}$ lanthanide hydrated ion. The $\{SbW_8O_{30}\}$ unit can be viewed as a $\{B\text{-}\beta\text{-}SbW_9O_{33}\}$ unit removing a $\{WO_6\}$ octahedron with three terminal oxo ligands (Fig. S3). Considering that the $\{B\text{-}\alpha\text{-}SbW_9O_{33}\}$ is used as the precursor, the tetravacant $\{B\text{-}\beta\text{-}SbW_8O_{30}\}$ is probably formed through the isomerization of $\{B\text{-}\alpha\text{-}SbW_9O_{33}\}$ to $\{B\text{-}\beta\text{-}SbW_9O_{33}\}$ followed by the removal of a single tungstate fragment (Scheme 1a). The similar tetravacant $\{B\text{-}\beta\text{-}AsW_8O_{30}\}$ species have ever been reported,[23] but the $\{B\text{-}\beta\text{-}SbW_8O_{30}\}$ unit in compound **1** is observed for the first time. In this POM fragment, all W centers display a hexa-coordinated octahedral environment. The W–O bond lengths are in the range of 1.65(2) ~ 2.35(1) Å, and the O–W–O angles range from 86.5(6)° to 175.6(6)°. In the metal-organic $\{WO_2(pic)\}$ units, the W center shows a hexa-coordinated environment with two O atoms derived from the $\{SbW_8O_{30}\}$ cluster, one O and one N atom derived from the 2-picolinic acid, and two terminal O atoms. The W–O bond lengths are in the range 1.648(2) ~ 2.236(2) Å, W-N bond lengths are in the range 2.297(1) ~ 2.345(2) Å, and the bond angles of O–W–O/N vary from 93.2(7)° to 14.5(7)°. Both La centers exhibit a nine-coordinated environment but possess different coordinated O atoms. La(1) is surrounded by two O atoms derived from one $\{SbW_8O_{30}\}$ unit (O(26), O(61)), two O atoms derived from two $\{WO_2(pic)\}$ units (O(2), O(48)), two O atoms derived from the adjacent $\{SbW_8O_{30}\}$ cluster (O(49), O(45)), and three coordinated water molecules (O(1W), O(2W), O(3W)). La(2) coordinates with five O atoms derived from the polyoxoanion (O(47), O(12), O(50), O(13), O(15)), two O atoms derived from two $\{WO_2(pic)\}$ units (O(32), O(3)) and one coordinated water molecule (O(4W)). The La-O bond lengths are in the range of 2.398(2) ~ 2.790(2) Å and the O-La-O angles vary from 68.1(5) to 139.3(5)°. Based on above connection modes, the basic structural unit of the polyoxoanion of **1** can be viewed as a sandwich-type cluster, in which two metal-organic $\{WO_2(pic)\}$ moieties and two La hydrated ions are sanwiched by two tetravacant $\{B\text{-}\beta\text{-}SbW_8O_{30}\}$ units (Fig. 1). Furthermore, such basic sandwich-type clusters are further linked by the $\{La(1)(H_2O)_3\}$ fragments to form a 1-D helical chain along *a* axis (Fig. 2a and Fig. S4).

In the packing arrangement, all these 1-D POM chains are parallel with each other and closely stacked together along *a* axis *via* $\pi\ldots\pi$ interactions among the pyridine groups decorated on the inorganic chains. The vertical distance between adjacent pyridine groups is ca. 3.62 Å. Based on such stacking mode, compound **1** exhibits a 3-D supramolecular framework with a 1-D channels along *a* axis (Fig. 2b). The Na cations and crystalline water molecules reside in the interspaces of such 3-D supramolecular framework *via* extensive electrostatic forces and intermolecular interactions. It is also worth mentioning that the compound **1** crystallizes in a chiral space group, but the flack parameter is 0.46(1), suggesting that the right-handed and left-handed helical POM-based chains cocrystallize together in one crystal of compound **1** to form a racemate.

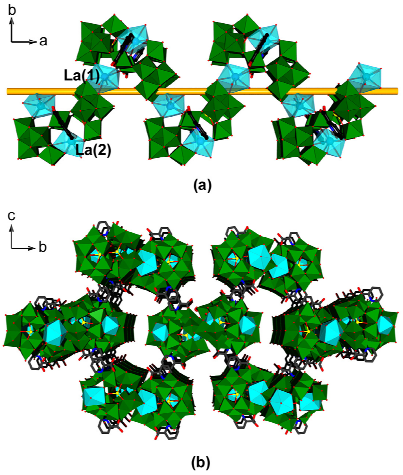

Fig. 2 (a) The helical chainlike structure based on the polyoxoanions of **1** extended along the *a* axis; (b) Packing arrangement of **1** viewed along the *a* axis. Hydrogen atoms, lattice water molecules and counter ions are omitted for clarity.

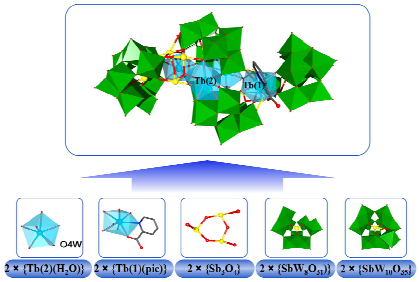

Fig. 3 Polyhedral and ball-and-stick view of the polyoxoanion of **3** and its basic building moieties

Single-crystal X-ray diffraction analyses indicate that compounds **3-5** contain the same polyoxoanion structure $[\{Ln(H_2O)\}\{Ln(pic)\}(Sb_3O_4)(SbW_8O_{31})(SbW_{10}O_{35})]_2^{24-}$ (Ln = Tb for **3**, Dy for **4** and Ho for **5**) (**Fig. 3**), although they possesses different components of cations and lattice water molecules. Herein, the polyoxoanion structure of compound **3** is described in details as the representative example. The polyoxoanion of **3** includes two $\{SbW_{10}O_{35}\}$ clusters, two $\{SbW_8O_{31}\}$ clusters, two $\{Sb_3O_4\}$ fragments, two $\{Tb(pic)\}$ units, and two $\{Tb(H_2O)\}$ hydrated ions.

Both $\{SbW_8O_{31}\}$ and $\{SbW_{10}O_{35}\}$ lacunary POM clusters partially keep the structural feature of {B-α-SbW_9O_{33}} unit (Fig. S3). Since the synthesis is originated from the {B-α-SbW_9O_{33}} precursors, the tetravacant {B-α-SbW_8O_{31}} moiety is probably formed by the removal of a single octahedral tungstate fragment on the {B-α-SbW_9O_{33}} unit. Such single tungstate fragment is further appended on the other undecomposed {B-α-SbW_9O_{33}} unit, forming the {B-α-$SbW_{10}O_{35}$} unit (Scheme 1b). The $\{Sb_3O_4\}$ unit contains a six-member ring formed by three Sb centers and three bridging O atoms. Each Sb center shows the distorted tetrahedral mode with three O atoms and a lone pair of electrons. The bond lengths of Sb-O in the $\{Sb_3O_4\}$ fragment range from 2.007(2) to 2.238(1) Å, which are slightly longer than those of Sb-O (Sb-O: 1.948(2) ~ 2.049(1) Å) in the center of lacunary POM units. It is worth mentioning that the trinuclear Sb cluster has ever been observed in the well-known $[Sb_9W_{21}O_{86}]^{19-}$ polyoxoanion, in which the three Sb centers are linked by one u_3-O bridge in the $\{Sb_3O_7\}$ unit.[33] In this case, however, the $\{Sb_3O_4\}$ units show a six-member-ring type structural feature, representing a new type of $\{Sb_3\}$ moiety. In the polyoxoanion of **3**, there are two types of Tb centers. Tb(1) center exhibits an eight-coordinated mode completed by two O atoms from the $\{SbW_8O_{31}\}$, two O atoms from the $\{SbW_9O_{33}\}$, two O atoms from the $\{Sb_3O_4\}$, and one O atom as well as one N atom from the picolinate ligand, respectively. The bond lengths of Tb(1)-O range from 2.294(1) to 2.436(1) Å. The bond length of Tb(1)-N is 2.586(1) Å. The bond angles of O-Tb(1)-O/N ranged from 70.9(5) to 141.4(5)°. Tb(2) center also displays an octa-coordinated environment with six O atoms derived from two $\{SbW_8O_{31}\}$ units, one O atom from the $\{Sb_3O_4\}$ unit and one terminal water ligand. The bond lengths of Tb(2)-O are in the range 2.286(1) ~ 2.659(1) Å. The bond angles of O-Tb(2)-O were distributed in 73.2(5) ~ 147.6(5)°. Based on above coordination modes, each $\{SbW_8O_{31}\}$ and $\{SbW_{10}O_{35}\}$ unit are connected by one $\{Sb_3O_4\}$ fragment and one $\{Tb(pic)\}$ moiety, forming a $[\{Tb(pic)\}(Sb_3O_4)(SbW_8O_{31})(SbW_{10}O_{35})]^{15-}$ unit (Fig. S5a). Then, such two units are further fused together via the connections between two $\{SbW_8O_{31}\}$ units and two $\{Tb(2)(H_2O)\}$ units (Fig. 3 and Fig. S5b).

Fig. 4. (a) Normalized excitation and emission spectra (λ_{ex}=275nm) of **Tb-3**; **(b)** normalized excitation and emission spectra (λ_{ex}=277nm) of **Dy-4**.

Photoluminescent properties

The introduction of lanthanide ions into the POM-based clusters may endow such compounds with potentially photoluminescent property. In this case, the luminescent properties of compounds **Tb-3** and **Dy-4** were detected as the representative examples. Before measurement, the phase purity of the samples were confirmed by the PXRD experiments (Fig. S14-15). The excitation spectra and the emission spectra of **Tb-3** and **Dy-4** were recorded at ambient temperature (**Fig. 4**). For compound **Tb-3**, the excitation peak maximum at 275 nm was measured by monitoring the Tb(III) emission at 544 nm. No other excitation peaks have been found in the UV region, suggesting that the sensitization of Tb(III) ions may not involve the POM-centered LMCT states.[34] As shown in Fig. 4a, the emission spectra of **Tb-3** consists of one strong green band centered at 544 nm and three weak lines centered at 489, 583, and 621 nm, respectively. The former emission line corresponds to the $^5D_4 \rightarrow {}^7F_5$ transition, while the latter are attributed to the $^5D_4 \rightarrow {}^7F_6$, $^5D_4 \rightarrow {}^7F_4$, and $^5D_4 \rightarrow {}^7F_3$ transitions of the Tb^{3+}ions, respectively.[34] For compound **Dy-4**, the excitation peak maximum at 277 nm was measured by monitoring the Dy(III) emission at 576 nm. Similar to **Tb-3**, no other excitation peaks were found in the UV region either. The characteristic high-intensity emission peak at 576 nm and two low-intensity emission peaks at 480 and 665nm correspond to the $^5D_0 \rightarrow {}^7F_1$, $^4F_{9/2} \rightarrow {}^6H_{15/2}$, and $^4F_{9/2} \rightarrow {}^6H_{11/2}$ transitions of Dy^{3+} ions, respectively (Fig. 4b).[35]

Based on the polyoxoanion structure of **Tb-3** and **Dy-4**, there may exist two contradictory structural factors to influence the final photoluminescent properties. In one aspect, partial Ln centers is coordinated with pic ligands, which can usually sensitize and promote the emission of Ln luminescence. In another aspect, however, the Ln-POMs that contain Ln-O-W bond angles of approximately 150° may allow for effective d^1 hopping through fπ–pπ–dπ orbital mixing, leading to the effective fluorescence quenching.[5,34] In the polyoxoanion structures of **Tb-3** and **Dy-4**, there are two types of Ln centers. The Ln(1) center is coordinated with the pic ligands. Two of the five Ln(1)-O-W bridges (corner-sharing linkage) possess the bond angles of 150-156° (Fig. S6a), which will be obviously insufficient for quenching the emission of Ln(1) luminescence sensitized by the pic ligands. The Ln(2) center exhibits the eight-coordinated environment with seven O atoms derived from POM units and one terminal water ligand (Fig. S6b). However, four of the seven Ln(2)-O-W bridges are involved in an edge-sharing mode with smaller Ln(2)-O-W angles in the range of 92-122°. Two of the three Ln(2)-O-W corner-sharing linkages with the Ln-O-W bond angles of ca. 150°, together with the coordinated water molecule, may led to less efficient luminescence quenching,[34,36] especially considering that the disadvantageous linkages and/or bonds just occupy 37.5% in the Ln(2) center. Thus, both compound **Tb-3** and **Dy-4** exhibit evident photoluminescent properties.

Conclusions

In summary, we herein reported five new polynuclear metal-oxo clusters, which are isolated from the reaction systems containing dynamic {B-α-SbW_9O_{33}} POM precursors, Ln^{3+} ions, organic pic ligand, and/or inorganic Sb^{3+} ions. The five compounds exhibit two types of new polyoxoanion structures, both representing the unprecedented metal-oxo clusters based on the {SbW_9O_{33}} building block and its derivatives. In comparison to the similar reaction systems containing {B-α-AsW_9O_{33}} POM precursors, the change of central heteroatoms of the POM building blocks did induce new assembling species of polynuclear metal-oxo clusters. Furthermore, the introduction of Ln^{3+} ions into the final clusters endow the compounds with various luminescent properties. It can be envisioned that changing the auxiliary organic and inorganic ligands, and tuning the central heteroatoms of the dynamic {XW_9O_{33}} building blocks pave new ways to design and synthesis of new polynuclear metal-oxo clusters. During the synthesis, exploring effective methods to introduce more Ln^{3+} ions into these polyoxoanion structures may suggest a new direction to obtain excellent luminescent materials. This work is ongoing in our research team.

Experimental

Materials and physical measurements

All chemicals were commercially purchased and used without further purification. $Na_9[B\text{-}\alpha\text{-}SbW_9O_{33}]\cdot 19.5H_2O$ was synthesized according to the literature and characterized by FT-IR spectrum.[36] Elemental analyses (C, N) were performed on a Perkin-Elmer 2400 CHN elemental analyzer. Li, Na, K, Ln, W, Sb were determined by a Leaman inductively coupled plasma (ICP) spectrometer. The FT-IR spectra were recorded on a Mattson Alpha-Centauri spectrometer with KBr pellets in the range of 4000–400 cm^{-1}. TG analyses were performed on a Pyris Diamond TG instrument in flowing N_2 with a heating rate of 10°C min^{-1}. The solid-state emission/excitation spectra were measured on a SPEX FL-2T2 spectrofluorimeter equipped with a 450 W xenon lamp as the excitation source. The capillary electrophoretic experiments were performed in a capillary electrophoretic apparatus (CL1020 Beijing Cailu Science Apparatus, China) under 22 °C cooling air with the UV detector.

Synthesis

$[Ln_2(H_2O)_4\{WO_2(pic)\}_2(SbW_8O_{30})_2]^{10-}$ (Na_4Li_6**[La-1]**$\cdot 28H_2O$, Na_3Li_7**[Pr-2]**$\cdot 17H_2O$)

La-1 was synthesized as follows: $La(NO_3)_3\cdot 6H_2O$(0.217g, 0.50 mmol) was dissolved into 20 mL distilled water. After that, 2-picolinic acid (0.123g, 1.00mmol) was added with vigorous stirring, followed by $Na_9[SbW_9O_{33}]\cdot 19.5H_2O$ (1.431g, 0.50 mmol) being added to the above solution. The solution became white turbid mixture, which was stirred fiercely until it became clear again. Then LiCl (0.848g, 20.00mmol) was added to the solution and stirred for 5 minutes at 90 °C. The pH value of this system was adjusted to 5.0 with 1 M HCl aqueous solution. The turbid solution was stirred for 3 h at 90 °C, cooled down to room temperature and filtered for crystallization at room temperature. Colorless column-like crystals of the compound **La-1** were isolated in a week. Yield: 39 % based on W. Elemental analysis for $C_{12}H_{72}N_2La_2Na_4Li_6O_{100}Sb_2W_{18}$, Calcd (%): C 2.48, N 0.48, Na 1.58, Li 0.72, La 4.78, Sb 4.19, W 56.97; Anal found(%): C 2.40, N 0.42, Na 1.52, Li 0.69, La 4.68, Sb 4.09, W 55.89. FT-IR (KBr pellet): ν = 3391(s), 1634(s), 1478 (m), 1446(m), 1379(s), 1301(m), 1259(m), 1170(m), 939(s), 858(s), 804(m), 652(w) and 455(w) cm^{-1}.

Pr-2 was obtained by the same way as **La-1**, except that $La(NO_3)_3\cdot 6H_2O$ was replaced by $Pr(NO_3)_3\cdot 6H_2O$ (0.218g, 0.50mmol). Colorless block crystals of the compound **Pr-2** were obtained with yield 32% (based on W). Elemental analysis for $C_{12}H_{50}N_2Pr_2Na_8Li_7O_{89}Sb_2W_{18}$ Calcd (%): C 2.57, N 0.50, Na 1.23, Li 0.87, Pr 5.03, Sb 4.35, W 59.11; Anal found(%): C 2.50, N 0.41, Na 1.12, Li 0.83, Pr 4.91, Sb 4.26, W 58.32. FT-IR (KBr pellet): ν = 3393(s), 1636(s), 1480(m), 1450(m), 1379(s), 1305(m), 1262(m), 1172(m), 941(s), 860(s), 805(m), 655(w) and 457 cm^{-1}(w).

$[\{Ln(H_2O)\}\{Ln(pic)\}(Sb_3O_4)(SbW_8O_{31})(SbW_{10}O_{35})]_2^{24-}$ ($K_2Na_6Li_{16}$**[Tb-3]**$\cdot 63H_2O$, Na_9Li_{15}**[Dy-4]**$\cdot 61H_2O$, Na_7Li_{17}**[Ho-5]**$\cdot 53H_2O$)

Tb-3 was synthesized as follows: $Tb(NO_3)_3\cdot 6H_2O$(0.227g 0.50mmol) was dissolved in 10 mL distilled water, and then 2-picolinic acid (0.123 g, 1.00mmol) was added with vigorous stirring. After that, $Na_9[SbW_9O_{33}]\cdot 19.5H_2O$ (2.0 g, 0.71 mmol) was added to the above solution. Plenty of precipitation appeared immediately in the solution, but it can be dissolved again after vigorous stirring for several minutes. When hydrochloric acid (12 M, 0.25 mL) containing Sb_2O_3 (0.146g, 0.50mmol) was dropwise added into above solution, the pH of the mixture was carefully adjusted to 6.5 with 1 M K_2CO_3 solution and 1 M HCl aqueous solution. Then LiCl (0.848g, 20.00mmol) was added to the solution, heated at 90 °C with vigorous stirring for 1h, and then cooled to room temperature. The filtrate was kept at room temperature for slow evaporation. Colorless block crystals of **Tb-3** were isolated after three days with the yield of 49% (based on W). Elemental analysis for $C_{12}H_{138}N_2Tb_4K_2Na_6Li_{16}O_{209}Sb_{10}W_{36}$, Calcd (%): C 1.16, N 0.23, K 0.63, Na 1.11, Li 0.89, Tb 5.10, Sb 9.78, W 53.14; Anal found(%): C 1.10, N 0.18, K 0.57, Na 1.06, Li 0.34, Tb 4.99, Sb 9.48, W 52.67. FT-IR data: (KBr pellet): ν = 3420 (s), 1621(s), 1581(m), 1466(w), 1414(s), 961(s), 899(s), 834(m), 797(m), and 700 cm^{-1}(w).

The syntheses of **Dy-4** and **Ho-5** were similar to that of **Tb-3** except that $Tb(NO_3)_3\cdot 6H_2O$ precursor was substituted by $Dy(NO_3)_3\cdot 6H_2O$ (0.228g, 0.50mmol) and $Ho(NO_3)_3\cdot 6H_2O$ (0.230g, 0.50mmol), respectively. Colorless block crystals of **Dy-4** were obtained after 3 days with the yield of 32% (based on W). Elemental analysis for $C_{12}H_{134}N_2Dy_4Na_9Li_{15}O_{207}Sb_{10}W_{36}$, Calcd (%): C 1.16, N 0.23, Na 1.67, Li 0.84, Dy 5.24, Sb 9.81, W 53.31; Anal found(%): C 1.12, N 0.19, Na 1.32, Li 0.76, Dy 5.10, Sb 10.02, W 52.10. FT-IR data(KBr pellet): ν = 3415(s), 1617(s), 1586(m), 1463(w), 1413(s), 961(s), 896(s), 836(m), 797(m) and 702 cm^{-1}(w). Colorless block crystals of **Ho-5** were obtained after 3 days with the yield of 42% (based on W). Elemental analysis for $C_{12}H_{118}N_2Ho_4Na_7Li_{17}O_{199}Sb_{10}W_{36}$, Calcd (%): C 1.18, N 0.23, Na 1.31, Li 0.96, Ho 5.39, Sb 9.94, W 54.03; Anal found(%): C 1.12, N 0.20, Na 1.03, Li 0.86, Ho 5.31, Sb 9.88, W 53.74. FT-IR (KBr pellet): v = 3419(s), 1619(s), 1583 (m), 1465(w), 1413(s), 960(s), 898(s), 835(m), 796(m), 701 cm^{-1}(w).

X-Ray crystallography

The crystal data for five compounds were collected on the Bruker Smart Apex CCD diffractometer. Suitable crystals were put in a glass tube using petroleum jelly and transferred to the goniostat. Data collection was performed at 296 K with graphite-monochromatic Mo Kα radiation (λ = 0.71073 Å). ω-2θ scan was applied to collect their diffraction points. A multi-scan absorption correction was applied. The crystal structures of **1-5** were solved by the direct method and refined by a full-matrix least-squares method on F^2 using the *SHELX-97* crystallographic software package.[38] During the refinement, the non-hydrogen atoms were refined anisotropically except partial counter cations and lattice water molecules. All H atoms on C atoms were fixed in calculated positions. H atoms on coordinated water molecules and lattice water molecules cannot be found from the residual peaks and were directly included in the final molecular formula. During the refinement of **1-5**, a series of restraint commands were used to refine a few of heavy metal centers, all the oxygen atoms on POM clusters and the C and N atoms on organic ligands, which led to high restraint values. The counter Na^+ cations and lattice water molecules

were assigned by the following strategies: (i) The distance of Na-O should be in the range of 2.2~3.0 Å; (ii) The distance of Na…Na should be longer than 3.0 Å; (iii) The distance of O…O should be longer than 2.5 A; (iv) The distance of O…O less than 2.4 Å should be one full-occupancy H_2O molecule with two possible disordered positions; (v) All Na^+ centers should possess similar thermal parameters, while all H_2O molecules should possess similar thermal parameters also. When rest counter-cations and lattice water molecules cannot be clearly assigned from the weak residual peaks, the SQUEEZE program[39] was further used to remove the contribution of rest weak reflections and the crystal data were refined with new hkl files generated by SQUEEZE calculation. Based on the charge-balance consideration, elemental analysis, TG analysis and the SQUEEZE calculation results, the rest counter cations and lattice water molecules were directly included in the final molecular formula. The detailed crystal data and structure refinement for **1 - 5** are given in Table 1. Selected bond lengths and angles of **1 - 5** are listed in Table S2 - S11, respectively.

Acknowledgement

This work was supported by the National Natural Science Foundation of China (grant nos. 21201032, and 21471028) and the Fundamental Research Funds for the Central Universities (2412015KJ012).

†Electronic supplementary information (ESI) available: Additional crystal structure figures, crystal data, TG, FT-IR and PXRD. CCDC 1041870 (La-1), 1041872 (Pr-2), 1041869 (Tb-3), 1041871 (Dy-4), 1041873 (Ho-5). For ESI and crystallographic data in CIF or other electronic format see DOI: 10.1039/xxxxxxxxx.

Notes and references

Address: [a]Key Laboratory of Polyoxometalate Science of Ministry of Education, Faculty of Chemistry, Northeast Normal University, Renmin Street No.5268, Changchun, Jilin, 130024, P. R. China. *Corresponding authors. E-mail addresses: wangyh319@nenu.edu.cn (Y.-H. Wang) and zanghy100@nenu.edu.cn (H.-Y. Zang)

1. A. Müller, F. Peters, M. T. Pope and D. Gatteschi, *Chem. Rev.*, 1998, **98**, 239.
2. A. Müller and P. Gouzerh, *Chem. Soc. Rev.*, 2012, **41**, 7431.
3. S. T. Zheng and G. Y. Yang, *Chem. Soc. Rev.*, 2012, **41**, 7623.
4. O. Oms, A. Dolbecq and P. Mialane, *Chem. Soc. Rev.*, 2012, **41**, 7497.
5. C. Ritchie, E. G. Moore, M. Speldrich, P. Kögerler and C. Boskovic, *Angew. Chem. Int. Ed.*, 2010, **49**, 7702.
6. H. N. Miras, J. Yan, D.-L. Long and L. Cronin, *Chem. Soc. Rev.*, 2012, **41**, 7403.
7. X. J. Feng, Y. G. Li, Z. M. Zhang and E. B. Wang, *Acta Chim. Sinica*, 2013, **71**, 1575.
8. (a) P. Huang, C. Qin, Z. M. Su, Y. Xing, X. L. Wang, K. Z. Shao, Y. Q. Lan and E. B. Wang, *J. Am. Chem. Soc.*, 2012, **134**, 14004; (b) X. B. Han, Z. M. Zhang, T. Zhang, Y. G. Li, W. B. Lin, W. S. You, Z. M. Su and E. B. Wang, *J. Am. Chem. Soc.,* 2014, **136**, 5359.
9. S. G. Mitchell, C. Streb, H. N. Miras, T. Boyd, D. L. Long and L. Cronin, *Nat. Chem.*, 2010, **2**, 308.
10. P. C. Yin, D. Li and T. B. Liu, *Chem. Soc. Rev.*, 2012, **41**, 7368.
11. K. Wassermann, M. H. Dickman and M. T. Pope, Angew. *Chem. Int. Ed. Engl.*, 1997, **36**, 1445.
12. (a) W. L. Chen, Y. G. Li, Y. H. Wang, E. B. Wang and Z. M. Su, *Dalton Trans.*, 2007, 4293; (b) X. J. Feng, H. Y. Han, Y. H. Wang, L. L. Li, Y. G. Li and E. B. Wang, *CrystEngComm.*, 2013, **15**, 7267.
13. (a) H. Y. Zang, A. R. dela Oliva, H. N. Miras, D. L. Long, R. T. McBurney, L. Cronin, *Nat. Commun.*, 2014, **5**, 3715; (b) M. D. Symes, P. J. Kitson, J. Yan, C. J. Richmond, G. J. T. Cooper, R. W. Bowman, T. Vilbrandt and L. Cronin, *Nat. Chem.*, 2012, **4**, 349.
14. J. P. Wang, P. T. Ma, J. Li, H. Y. Niu and J. Y. Niu, *Chem. Asian. J.*, 2008, **3**, 822.
15. K. Y. Cui, F. Y. Li, L. Xu, B. B. Xu, N. Jiang, Y. C. Wang and J. P. Zhang, *Dalton Trans.*, 2012, **41**, 4871.
16. G. Al-Kadamany, S. S. Mal, B. Milev, B. G. Donoeva, R. I. Maksimovskaya, O. A. Kholdeeva and U. Kortz, *Chem. Eur. J.*, 2010, **16**, 11797.
17. M. Ibrahim, S. S. Mal, B. S. Bassil, A. Banerjee and U. Kortz, *Inorg. Chem.*, 2011, **50**, 956.
18. G. L. Xue, J. Vaissermann and P. Gouzerh, *J. Cluster. Sci.*, 2002, **13**, 3.
19. R. R. Cui, H. L. Wang, X. Y. Yang, , S. H. Ren, H. M. Hu, F. Fu, J. W. Wang and G. L. Xue, *Chin. J. Chem.*, 2007, **25**, 176.
20. T. Yamase, K. Fukaya, H. Nojiri and Y. Ohshima, *Inorg. Chem.*, 2006, **45**, 7698.
21. D. Drewes, B. Piepenbrink and M. Krebs, Z. Anorg. *Allg. Chem.*, 2006, **632**, 534.
22. F. Hussain, R. W. Gable, M. Speldrich, P. Kögerlerb and C. Boskovic, *Chem. Commun.*, 2009, 328.
23. C. Ritchie and C. Boskovic, *Cryst. Growth Des.*, 2010, **10**, 488.
24. C. Ritchie, M. Speldrich, R. W. Gable, L. Sorace, P. Kögerler, and C. Boskovic, *Inorg. Chem.*, 2011, **50**, 7004.
25. C. Ritchie, C. E. Miller and C. Boskovic, *Dalton Trans.*, 2011, **40**, 12037.
26. M. Vonci, F. A. Bagherjeri, P. D. Hall, R. W. Gable, A. Zavras, R. A. J. O'Hair, Y. P. Liu, J. Zhang, M. R. Field, M. B. Taylor, J. D. Plessis, G. Bryant, M. Riley, L. Sorace, P. A. Aparicio, X. López, J. M. Poblet, C. Ritchie and C. Boskovic, *Chem. Eur. J.*, 2014, **20**, 14102.
27. (a) F. Hussain, F. Conrad and G. R. Patzke, *Angew. Chem. Int. Ed.*, 2009, **48**, 9088; (b) F. Hussain and G. R. Patzke, *CrystEngComm,* 2011, **13**, 530.
28. J. Yan, J. Gao, D. L. Long, H. N. Miras and L. Cronin, *J. Am. Chem. Soc.*, 2010, **132**, 11410.
29. W. C. Chen, H. L. Li, X. L. Wang, K. Z. Shao, Z. M. Su and E. B. Wang, *Chem. Eur. J.*, 2013, **19**, 11007.
30. L. C. Zhang , H. Xue, Z. M. Zhu, Q. X. Wang, W. S. You, Y. G. Li and E. B. Wang, *Inorg. Chem. Commun.*, 2010, **13**, 609.
31. R. X. Tan, X. H. Pang, Y. L. Ren, X. H. Wang, and R. Li, *Z. Anorg. Allg. Chem.*, 2011, **637**, 1178.
32. (a) S. Himeno, I. Kitazumi, M. Takamoto, Y. Nakashima, *Talanta* 2003, **61**, 591; (b) S. Himeno, E. Kitano, M. Kanaya, M. Takamoto, *Talanta* 2007, **71**, 822.
33. J. Fischer, L. Ricard and R. Weiss, *J. Am. Chem. Soc.*, 1976, **98**, 3050.
34. T. Yamase, *Chem. Rev.,* 1998, **98**, 307.
35. Y. Kikukawa, S. Yamaguchi, Y. Nakagawa, K. Uehara, S. Uchida, K. Yamaguchi and N. Mizuno, *J. Am. Chem. Soc.*, 2008, **130**, 15872.
36. A. Beeby, I. M. Clarkson, R. S. Dickins, S. Faulkner, D. Parker, L. Royle, A. S. de Sousa, J. A. G. Williams and M. Woods, *J. Chem. Soc. Perkin Trans.*, 1999, **2**, 493.
37. M. Bösing, I. Loose, H. Pohlmann and B. Krebs, *Chem. Eur. J.*, 1997, **3**, 1232.
38. (a) G. M. Sheldrick, SHELXL 97, Program for Crystal Structure Refinement, University of Gőttingen, Germany, 1997; (b) G. M. Sheldrick, SHELXL 97, Program for Crystal Structure Solution, University of Gőttingen, Germany, 1997.
39. A. L. Spek, *Acta Cryst.*, 2015, **C71**, 9.

Table 1 Crystal data and structure refinement of **1 - 5**

Compounds	**La-1**	**Pr-2**	**Tb-3**	**Dy-4**	**Ho-5**
Empirical formula	$C_{12}H_{72}N_2La_2Na_4Li_6O_{100}Sb_2W_{18}$	$C_{12}H_{50}N_2Pr_2Na_3Li_7O_{89}Sb_2W_{18}$	$C_{12}H_{138}N_2Tb_4K_2Na_6Li_{16}O_{209}Sb_{10}W_{36}$	$C_{12}H_{134}N_2Dy_4Na_9Li_{15}O_{207}Sb_{10}W_{36}$	$C_{12}H_{118}N_2Ho_4Na_7Li_{17}O_{199}Sb_{10}W_{36}$
Formula weight	5808.93	5598.71	12454.20	12416.31.22	12249.81
λ/Å	0.71073	0.71073	0.71073	0.71073	0.71073
T/K	298(2) K	298(2) K	296(2) K	298(2) K	296(2) K
Crystal system	Orthorhombic	Orthorhombic	Monoclinic	Triclinic	Triclinic
Space group	*P2(1)2(1)2(1)*	*P2(1)2(1)2(1)*	P2(1)/n	*P-1*	*P-1*
a/Å	18.6089(17)	18.333(4)	15.1737(14)	14.1382(15)	14.5090(15)
b/Å	24.713(2)	24.500(5)	23.009(2)	20.272(2)	20.299(2)
c/Å	25.418(2)	25.269(5)	32.566(3)	20.946(2)	21.776(2)
α/°	90.000	90.000	90.000	101.760(2)	72.271(2)
β/°	90.000	90.000	77.005	107.002(2)	70.725(2)
γ/°	90.000	90.000	90.000	105.855(2)	74.329(2)
V/Å^3	11689.5(19)	11349(4)	11078.7(17)	5253.4(10)	5662.9(10)
Z	4	4	2	1	1
D_{calc}/Mg m^{-3}	3.301	3.277	3.733	3.925	3.592
μ/mm^{-1}	18.916	19.571	21.217	22.413	20.862
F(000)	10272	9816	10964	5458	5366
Data/restraints/parameters	20667 / 258 / 1041	19755 / 770 / 975	19489 / 531 / 1093	18422 / 576 / 1028	19926 / 487 / 1057
GOF on F^2	0.984	0.903	0.941	1.011	1.050
$R_1(I > 2\sigma(I))$[a]	R_1= 0.0557	R_1=0.0823	R_1= 0.0550	R_1=0.0619	R_1=0.0605
wR_2[b]	*wR2* = 0.0934	wR_2 =0.1538	*wR2* = 0.1405	wR_2 = 0.1662	wR_2 = 0.1588

Note: [a]$R_1 = ||F_0|-|F_c||/|F_0|$; [b]$wR_2 = [w(F_0^2-F_c^2)^2]/[w(F_0^2)^2]^{1/2}$

Table of Contents